Journal of Neurology (2019) 266:1743–1755
https://doi.org/10.1007/s00415-019-09328-7

ORIGINAL COMMUNICATION

Pathologic and MRI analysis in acute atypical inflammatory demyelinating lesions

Xavier Ayrignac[1,2] · Valérie Rigau[3] · Benoit Lhermitte[4] · Thierry Vincent[5] · Nicolas Menjot de Champfleur[6] · Clarisse Carra-Dalliere[1] · Mahmoud Charif[1] · Nicolas Collongues[7] · Jérôme de Seze[7] · Sonia Hebbadj[8] · Guido Ahle[9] · Hélène Oesterlé[10] · François Cotton[11] · Françoise Durand-Dubief[12] · Romain Marignier[12] · Sandra Vukusic[12] · Frédéric Taithe[13] · Mikael Cohen[14] · Anne-Marie Guennoc[15] · Anne Kerbrat[16] · Gilles Edan[16] · Béatrice Carsin-Nicol[17] · Thibaut Allou[18] · Denis Sablot[18] · Eric Thouvenot[19] · Aurélie Ruet[20] · Laurent Magy[21] · Marie-Paule Boncoeur-Martel[22] · Pierre Labauge[1] · Stéphane Kremer[8]

Received: 28 January 2019 / Revised: 12 April 2019 / Accepted: 16 April 2019 / Published online: 23 April 2019

Abstract

Background The diagnosis of atypical inflammatory demyelinating lesions can be difficult. Brain biopsy is often required to exclude neoplasms. Moreover, the relationship between these lesions and multiple sclerosis and NMOSD is not clear.

Objectives Our objectives were to describe radiological and pathological characteristics of patients with acute inflammatory demyelinating lesions.

Methods We retrospectively identified patients with brain biopsy performed for diagnostic uncertainty revealing a demyelinating lesion. A complete clinical, biological, radiological and pathological analysis was performed.

Results Twenty patients (15 with a single lesion) were included. MRI disclosed a wide range of lesions including infiltrative lesions (40%), ring-like lesion (15%) Baló-like lesion (15%) and acute haemorrhagic leukoencephalitis (20%). In spite of a marked heterogeneity, some findings were common: a peripheral B1000 hyperintense rim (70%), a slight oedema with mild mass effect (75%) and an open-rim peripheral enhancement (75%). Histopathology revealed that all cases featured macrophages distributed throughout, extensive demyelination, axonal preservation and absence of haemorrhagic changes. In the majority of cases, macrophages were the predominant inflammatory infiltrate and astrocytes were reactive and dystrophic. Aquaporin-4 staining was systematically preserved. After a mean follow-up of 5 years (1–12), 16/20 patients had a diagnosis of monophasic acute atypical inflammatory demyelinating lesion. One patient was diagnosed with MS and 3 with AQP4 negative NMOSD.

Discussion Although imaging findings in patients with atypical inflammatory demyelinating lesions are heterogeneous, some common features such as peripheral DWI hyperintense rim with open-rim enhancement and absence of oedema argue in favour of a demyelinating lesion and should preclude a brain biopsy. In this context, AQP4 staining is systematically preserved and argues against an AQP4-positive NMOSD. Moreover, long-term follow-up is characterized by low recurrence rate.

Keywords Atypical demyelinating lesions · Aquaporin-4 · Magnetic resonance imaging · Atypical inflammatory demyelinating syndrome · Immunopathology · Histopathology

Abbreviations

AHLE	Acute haemorrhagic leukoencephalitis
AQP4	Aquaporin-4
AIIDL	Atypical idiopathic inflammatory demyelinating lesion
CNS	Central nervous system
DWI	Diffusion-weighted imaging
FLAIR	Fluid attenuated inversion recovery
GFAP	Glial fibrillary acid protein
IgG	Immunoglobulin G
LFB	Luxol fast blue
MOG	Myelin oligodendrocyte glycoprotein
MS	Multiple sclerosis
NMO	Neuromyelitis optica
NMOSD	Neuromyelitis optica spectrum disorders
ON	Optic neuritis

✉ Xavier Ayrignac
xavier.ayrignac@yahoo.fr

Extended author information available on the last page of the article

Introduction

Atypical inflammatory demyelinating lesions of the central nervous system (CNS) are a heterogeneous group of demyelinating lesions with distinct clinical and magnetic resonance imaging (MRI) findings [1]. Even if some "characteristic" atypical brain lesions, such as Baló's disease or tumefactive demyelination, have been extensively reported, their relationship with multiple sclerosis (MS), notably in the absence of otherwise typical MS lesions, is still unclear [1]. Moreover, in some patients, for example with infiltrative lesions involving the corpus callosum, there are important differential diagnoses, including brain tumor. In these cases, brain biopsy is frequently needed [2, 3].

Additionally, similar atypical inflammatory demyelinating lesions, including pseudotumoral lesions, have been reported in patients with aquaporin-4 (AQP4-) and Myelin Oligodendrocyte Glycoprotein (MOG-) related neuromyelitis optica spectrum disorder (NMOSD) [4, 5]. This is of particular importance since evolution and treatment of MS and NMOSD are different. In this context, it has been suggested that a significant proportion of patients with atypical demyelinating lesions could be related to APQ4-NMOSD [6]. Indeed, in a previous series of 20 patients with CNS atypical demyelination and pathological evidence of an astrocytopathy, immunohistochemistry found a decrease of AQP4 staining in 90% of them, with presence of antibody directed against AQP4 in the serum in 78%.

The aim of our study is to describe the clinical, radiological and pathological characteristics of a series of patients with pathologically proven atypical idiopathic inflammatory demyelinating lesion (AIIDL) who underwent biopsy for diagnostic uncertainty.

Materials and methods

Cohort

This retrospective multicenter study included 20 patients from 9 French neurological departments. Inclusion criteria were: (1) acute or subacute onset of neurological deficit, (2) brain biopsy performed for diagnostic uncertainty revealing a demyelinating lesion as defined by the presence of large areas of demyelination assessed by loss of myelin content identified by Luxol fast blue (LFB) staining, (3) sufficient material for all the stainings, and (4) no alternative diagnosis (infection, systemic disease, neoplasm) identified during a mean follow-up of 5 years (min–max: 1.5–12 years) [7, 8]. All medical records of the patients were reviewed by a neurologist (XA) and the following data were recorded: previous medical history, including previous neurologic relapses, gender, age and clinical symptoms at onset. Finally, diagnosis at last follow-up was made according to current diagnosis criteria for MS and NMOSD [7, 8]. Four patients (patients 3–6) have been previously published [9].

Imaging

Brain MRI was obtained on either 1.5 or 3.0-T scanners. A neurologist (XA) and a neuroradiologist (SK) retrospectively analysed all the MRI. The analysis focused on T1- (pre- and post-gadolinium product injection), T2-, T2 gradient echo-, fluid attenuated inversion recovery (FLAIR) and diffusion-weighted imaging (DWI). The following data were recorded: number of lesions, location (cortical, juxtacortical, periventricular, corpus callosum involvement, posterior fossa involvement), presence of a peripheral hypointense (on T2-WI) or hyperintense (on DWI) rim, and type of gadolinium enhancement (peripheral open or closed enhancement, central enhancement) [10, 11]. The presence of oedema was recorded, and mass effect was classified as mild (mild sulcal effacement), moderate (ventricular impingement) or severe (subfalcial herniation) depending on location and degree of mass effect. According to the classification of atypical inflammatory demyelinating lesions, patients were classified as having either infiltrative lesions (large, ill-defined areas of T2 abnormalities), ring-like lesions (round lesions with ring-like enhancement), or Baló-like lesions (lesions with multiple concentric/alternating bands of signal intensity) [12]. Moreover, patients with radiological evidence of acute haemorrhagic lesions on susceptibility-weighted imaging were considered to have acute haemorrhagic leukoencephalitis (AHLE) [1]. Spinal cord MRI was available in 19 patients (95%).

Pathological analysis

Two experienced neuropathologists (VR and BL) blinded to the MRI and clinical data performed all the pathologic evaluations. Paraffin-embedded sections were stained using haematoxylin and eosin and Luxol-Fast-Blue (LFB: for the identification of myelin). Primary antibodies specific for GFAP (astrocytes), CD3 (T cells), CD8 (CD8 T cells), CD20 (B cells) and CD68 (microglia and macrophages) were used in routine practice in all the referring pathological departments. Additional immunohistochemical studies were systematically done using primary antibodies specific for immunoglobulin-G (IgG: mouse monoclonal, clone A57H, 1:100, Dako) and AQP4 (astrocytes: rabbit polyclonal 1:2000; Sigma-Aldrich).

Lesions were classified according to recent histological classification: they were considered to be active when macrophages/microglia were seen throughout lesions, or mixed active/inactive when they were mainly located at lesion border [11]. Demyelinating or post-demyelinating lesions were distinguished according to the presence (demyelinating) or absence (post-demyelinating) of LFB + degradation products within macrophages/microglia according to a recent pathological classification [13]. Astrocyte morphology was described according to previous characterization as follows: reactive astrocytes (with prominent processes), dystrophic astrocytes (small astrocytes with short and blunted processes) or Creutzfeldt–Peters cells (large astrocytes with abundant cytoplasm and fragmented nuclear inclusion) [6, 14–16]. Finally, we analysed the AQP4 immunohistochemical staining [6].

The study was approved by Montpellier University Hospital Ethical Committee (Q-2017-03-02) and was registered on ClinicalTrial.gov (NCT03121105).

Results

Clinical characteristics (Table 1)

Twenty patients were included (13 women/7 men). Mean age at onset was 42.4 years (20–67). Two patients had had previous neurological attacks (patient 1: visual symptoms and patient 20: recurrent bilateral optic neuritis) with a mean delay between the first attack and the recent episode of 2.5 years (2–3). The most common symptoms at onset were hemiparesis (50%) followed by aphasia (30%); 2 patients had seizures. Mean delay between onset of the symptoms and biopsy was 49 days (median: 24 days; 4–271). Three patients (15%) were admitted to intensive care unit, 2 of them rapidly died. Only patient 1 had, in addition to visual symptoms, evidence of a spinal cord involvement. His neurological status progressively worsened over few months and he died in a palliative care unit.

Nineteen out of 20 patients received intravenous methylprednisolone and/or oral steroids with tapering, followed by immunomodulatory/immunosuppressive treatments in 35% of them. During a mean follow-up of 5 years (1.5–12 years), 2 patients presented new symptoms; in both cases it was a severe unilateral optic neuritis (recurrent in 1). Of the 17 survivors, 13 (76%) were fully autonomous with no or few symptoms, whereas 4 (24%) had various degrees of disability. At the end of the follow-up, final diagnosis was monophasic AIIDL in 16 (80%), AQP4-negative NMOSD in 3, and an MS diagnosis was retrospectively done according to initial MRI findings in 1 patient.

Laboratory findings (Table 1)

All the patients had an extensive laboratory work-up to exclude systemic disease, infection, or neoplasm; it was systematically negative/normal. CSF abnormalities were found in 10/20 patients: elevated protein levels in 7 (mean 48 mg/dl; 20-118), pleocytosis in 2 (respectively, 6 and 38 cells/ml) and oligoclonal bands in 4. AQP4-IgG and MOG-IgG antibodies were systematically negative in the 13 and 11 tested cases (at the time of the initial screening or later).

Neuroimaging data (Table 2, Figs. 1, 2)

On MRI, lesions were heterogeneous. Eight patients (40%) had an infiltrative lesion, 3 had a ring-like lesion (15%) and 3 had Baló-like lesion (15%). Moreover, 4 patients (20%) had T2-Gradient Echo hypointensities: they were considered to have an acute haemorrhagic leukoencephalitis (AHLE). Finally, two patients had an unclassified lesion.

A single lesion was observed in 75% of the patients. The mean number of lesions in the 5 remaining patients was 7 (2–14 lesions per patient). Only patient 12 had lesions suggestive of MS (both enhancing and non-enhancing periventricular and cortical/juxtacortical lesions). Five patients (25%) had posterior fossa lesions including one patient with a single pontomesencephalic lesion in the absence of supratentorial lesions.

Lesions mainly involved white matter. They were frequently juxtacortical (90%) and periventricular (80%) with less frequent extension to cortex (35%) and deep grey matter (20%). Corpus callosum involvement was observed in 12 patients (60%), with a butterfly like pattern in 8 (40%). Fluffy lesions were not seen.

Oedema was present in 80% of the patients; mass effect was usually mild or moderate (87.5% of them), and rarely severe (12.5%). A T2 hypointense rim was seen in 15%. On DWI, a peripheral hyperintense rim was observed in 70% whereas central core was hyperintense and iso/hypointense in, respectively, 50% and 45% of cases. ADC images were available for 15 patients; 3 patients (20%) had central core hypointensities and 7 patients (47%) had peripheral hypointense rim. Four patients had T2* hypointensities suggestive of haemorrhage.

Gadolinium enhancement was systematically found. Enhancement was peripheral in 18/20 patients (90%) with open enhancement in 15 patients (75%) and a central, heterogeneous enhancement in 63%.

All but patient n° 17 had spinal cord MRI. It was normal in 17 patients and a single short partial myelitis was found in cases 1 and 19.

Table 1 Main characteristics of the patients

Patient number	Gender age at biopsy	Disease Duration (days)[a]	Previous neurologic history (delay, years)	Clinical symptoms	Protein level (mg/dl)	Cell count (/ml)	OCB/IgG index	Aqp4-/MOG-IgG	MRI diagnosis	F-up (years)	Treatment: acute/chronic	Diagnosis at follow-up
1	M, 63	119/30	visual symptoms (3 years)	Paraparesis, visual symptoms	98	< 3	neg/ND	ND/ND	Infiltrative	0.5	Steroids/none	Unknown/rapid death
2	M, 24	15/5	No	Left hemiparesis	50	< 3	neg/Nl	neg/neg	Other	8	Steroids/none	Monophasic AIIDL
3	F, 43	9/2	No	Left hemiparesis	45	< 3	ND/ND	neg/neg	Infiltrative	3	Steroids/none	Monophasic AIIDL
4	M, 47	35/10	No	Aphasia, right hemiparesis	42	< 3	neg/ND	ND/ND	Infiltrative	5	Steroids/none	Monophasic AIIDL
5	F, 20	2/32	No	Aphasia	20	6	neg/ND	neg/neg	Ring-like	7	Steroids/none	Monophasic AIIDL
6	M, 26	14/2	No	Left hemiparesis	30	< 3	pos/ND	neg/neg	Infiltrative	12	Steroids/none	NMOSD/severe left optic neuritis
7	F, 42	4/4	No	Right hemiparesis	30	3	neg/ND	neg/neg	AHLE	4	Steroids/terifl-unomide	Monophasic AIIDL
8	F, 55	8/11	No	Right hemiparesis	33	0	neg/Nl	neg/neg	ring-like	1	Steroids/none	Monophasic AIIDL
9	F, 20	5/23	No	Aphasia, auditory hallucinations	56	1	neg/ND	neg/neg	Balo-like	1.5	Steroids/none	Monophasic AIIDL
10	F, 37	29/14	No	Ataxia, right sensory loss	42	7	neg/Nl	ND/ND	Balo-like	4	Steroids/none	Monophasic AIIDL
11	F, 43	5/4	No	Headaches	24	4	neg/Nl	neg/neg	AHLE	2.5	Steroids/none	Monophasic AIIDL
12	F, 46	210/61	No	Partial seizures, aphasia, right hemiparesis	normal	38	pos/1.6	neg/neg	Balo-like	3	Steroids/mitoxantrone	MS/DIS + DIT at onset
13	F, 39	1/3	No	Right hemiparesis, aphasia, visual symptoms	36	3	pos/neg	neg/neg	Infiltrative	10	Steroids/MMF	Monophasic AIIDL
14	F, 33	55/3	No	Confusion	36	1	neg/ND	neg/ND	Infiltrative	5	Steroids/MMF	NMOSD/severe recurrent right optic neuritis
15	M, 67	5/2	No	Partial complex seizure, coma	55	1	neg/ND	ND/ND	Infiltrative	2	Steroids/none	Monophasic AIIDL
16	F, 30	3/4	No	Left hemiparesis	36	1	neg/ND	ND/ND	AHLE	0	Steroids/none	Unknown/rapid death
17	F, 64	29/16	No	Aphasia	38	1	neg/Nl	ND/ND	Ring-like	3	None/none	Monophasic AIIDL
18	F, 54	84/29	No	Unsteadiness, left hemiparesis	55	< 3	neg/Nl	ND/ND	Infiltrative	5	Steroids/mitoxantrone	Monophasic AIIDL

Table 1 (continued)

Patient number	Gender age at biopsy	Disease Duration (days)[a]	Previous neurologic history (delay, years)	Clinical symptoms	Protein level (mg/dl)	Cell count (/ml)	OCB/IgG index	Aqp4-/MOG-IgG	MRI diagnosis	F-up (years)	Treatment: acute/chronic	Diagnosis at follow-up
19	M, 35	50/34	No	Memory loss	118	24	pos/0.8	neg/neg	AHLE	3.5	Steroids/immunoglobulin, cyclophosphamide	Monophasic AIIDL
20	M, 62	2/3	Recurrent bilateral optic neuritis (2 years)	Tetraparesis, loss of arousal	64	6	neg/Nl	neg/ND	Other	0.5	Steroids/rituximab	NMOSD/rapid death

AIIDL acute idiopathic inflammatory demyelinating lesion, *OCB* oligoclonal bands, *MRI* magnetic resonance imaging; *ND* not done, *Nl* normal, *NMOSD* neuromyelitis optica spectrum disorder, *AHLE* acute haemorrhagic leukoencephalitis, *MS* multiple sclerosis; *DIS* dissemination in space, *DIT* dissemination in time, *MMF* Mycophenolate mofetil

[a]Delays between onset of the disease and MRI and then between MRI and biopsy are disclosed

Pathological analysis (Table 3, Fig. 3)

Six patients had been treated with steroids at the time of pathological analysis. Pathological analysis from biopsy ($n = 19$) or autopsy (patient 16) systematically disclosed active lesions with macrophages distributed throughout the lesion in all the cases. There were no significant differences between treated and untreated patients according notably to inflammatory infiltrate. Demyelination was extensive without perivenous distribution in all the cases. Axonal preservation suggested a primary demyelination. No haemorrhage was observed even in patients with T2* images suggestive of haemorrhagic changes. Within the lesion, foamy macrophages containing myelin debris were seen in 70% of the patients (Fig. 3a). Inflammatory infiltrate was usually marked (80%) with predominant macrophages (Fig. 3b) in all the patients. A T cell mild infiltrate (Fig. 3c) was present in most cases (70%), whereas B cells (Fig. 3d) were found in 20%. IgG deposits were observed in 61% of the patients (Fig. 3e); they were predominantly located in the parenchyma with perivascular reinforcement but without clear rosette aspect. Along with myelin debris, macrophages contained GFAP + material in 1 patient. Vascular hyalinization (Fig. 3f) and myelin vacuolation (Fig. 3g) were, respectively, seen in 4 (20%) and 6 (30%) patients. Granulocytes were seen in 4 patients (Fig. 3h). Astrocyte morphological analysis disclosed reactive astrocytes (Fig. 3i), dystrophic astrocytes (Fig. 3j) and Creutzfeldt–Peters cells (Fig. 3k) in 85, 60 and 35% of cases, respectively. AQP4 immunostaining disclosed normal or increased astrocyte immunoreactivity in all the patients (Fig. 3l).

Discussion

Our study confirms that, in patients requiring a pathological analysis for diagnostic uncertainties, MRI findings of atypical inflammatory demyelinating lesions can be strikingly heterogeneous. Indeed, patients could present with either infiltrative lesions with diffuse, ill-defined hyperintensities predominantly involving the corpus callosum or well-circumscribed juxtacortical ring-like lesions. Moreover, while contrast enhancement was homogeneous with an open-rim in most of the cases, it could be more heterogeneous with radiological evidence of haemorrhages in around 20%.

In spite of these discrepancies, some previously described characteristic features of inflammatory demyelinating lesions were confirmed. Indeed, oedema was usually mild (as compared to lesion size) with little or no mass effect in 80% of the patients (nearly 90% in previous series) [9–11]. Moreover, even if a T2 hypointense rim was seen in only 15% of our patients (42–45% of previously published patients with tumefactive lesions), a peripheral hyperintense DWI

Table 2 MRI characteristics of patients with acute idiopathic inflammatory demyelinating lesion

Characteristics	Whole cohort ($n=20$)	Infiltrative ($n=8$, 40%)	AHLE ($n=4$, 20%)	Ring-like ($n=3$, 15%)	Balo-like ($n=3$, 15%)	Unknown ($n=2$, 10%)
Lesion number						
Unique	15 (75%)	88%	50%	100%	67%	50%
Multiple	5 (25%)	12%	50%	None	33%	50%
MS typical lesions	1 (5%)	None	None	None	33%	None
Lesion topography						
Cortical	7 (35%)	25%	50%	33%	33%	50%
Juxtacortical	18 (90%)	88%	100%	100%	100%	50%
Periventricular	16 (80%)	100%	100%	33%	100%	None
Corpus callosum	12 (60%)	88%	75%	None	33%	None
Posterior fossa	5 (25%)	12%	75%	None	None	50%
Deep grey matter	4 (20%)	12%	75%	None	None	None
Butterfly aspect	8 (40%)	75%	50%	None	None	None
Oedema	16 (80%)	88%	100%	67%	67%	50%
Mass effect						
Mild	12 (75%)	75%	25%	67%	50%	50%
Moderate	2 (12.5%)	None	50%	None	None	None
Severe	2 (12.5%)	12%	25%	None	None	None
T2 hypointense rim	3 (15%)	38%	None	None	None	None
T2-GE hypointensity	3/19 (16%)	None	100%	None	None	None
DWI						
Core: hyperintense	50%	50%	50%	67%	None	100%
Core: iso/hypointense	45%	50%	50%	33%	67%	None
Peripheral rim	14 (70%)	75%	50%	67%	100%	50%
ADC ($n=15$ patients)						
Core hypo	3/15	1 patient	1 patient	1 patient	None	None
Peripheral hypo	7/15	3 patients	1 patient	2 patients	None	1 patient
Contrast enhancement	20 (100%)	100%	100%	100%	100%	100%
Core	13 (65%)	50%	75%	67%	33%	100%
Peripheral	18 (90%)	88%	100%	100%	100%	50%
Open-rim enhancement	15 (75%)	88%	75%	67%	67%	50%

AHLE acute haemorrhagic leukoencephalitis, *DWI* diffusion-weighted imaging, *ADC* apparent diffusion coefficient

rim was seen in 70% of the patients. [10, 17] This is in line with a previous series studying specifically DWI in atypical demyelinating lesions [18]. Finally, contrast enhancement was always seen with a nearly systematic peripheral rim (in 90%) that was open in 75% of the patients and frequent central enhancement (65%) [19]. Taken together, all these features argue for a demyelinating lesion and against a tumoral process. They should be considered in the management of patients presenting with acute/subacute neurological symptoms since, when present, brain biopsy brain biopsy should be avoided.

Many patients in our cohort had infiltrative lesions ($n=9/45\%$). This is in line with recent series on AIIDL that have reported a proportion of infiltrative lesions between 16% and 49% of the whole group. [12, 20] Indeed, these infiltrative lesions of the corpus callosum, notably those with butterfly like aspect, have a wide range of differential diagnoses, including lymphoma and glioblastoma. As a consequence, they more frequently require a biopsy than, for example, patients with suspected Baló lesion [21, 22]. In this context, 75% of our patients disclose an open-rim gadolinium enhancement whereas immunocompetent patients with primary CNS lymphoma and glioblastoma usually have a predominantly homogeneous or heterogeneous central enhancing pattern [23–25].

At the frontier between NMOSD and MS, non-MS non-NMOSD atypical demyelinating lesions share some pathological features common to both diseases [1, 2, 26]. Whereas in AQP4-positive NMOSD (an autoimmune astrocytopathy with secondary demyelination), main changes include granulocyte infiltrates, vascular hyalinization and myelin vacuolation associated with astrocyte loss and dystrophic

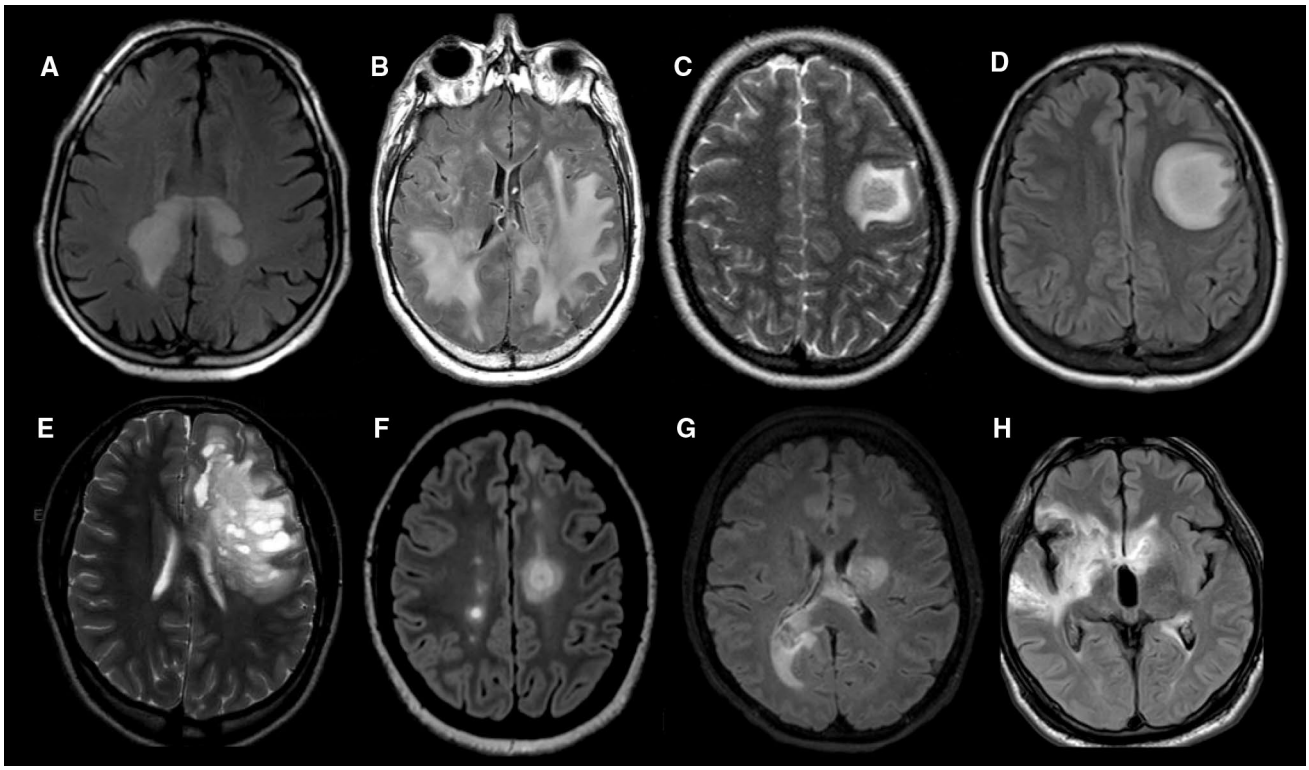

Fig. 1 Typical MRI. FLAIR (**a**, **b**, **d**, **f**, **g**), T2 (**c**, **e**) and T2-GRE (**h**) are disclosed. On MRI, the lesions disclosed a significant heterogeneity. We identified infiltrative (**a**, **b**), ring-like (**c**, **d**), and Baló-like (**e**, **f**) lesions. Some patients with evidence of haemorrhages were considered to have an acute haemorrhagic leukoencephalitis (**g**, **h**)

astrocytes, and in MS (a primary myelin disorder) most of these features are normally absent [27–29]. In patients with AIIDL, pathologic changes are usually similar to those seen in prototypic MS but marked astrocytic changes such as Creutzfeldt–Peters astrocytes or dystrophic changes are commonly seen [26]. Importantly, patients with all these atypical conditions have also been described in the context of AQP4-positive NMOSD [4, 5, 29–31]. In our series, pathological changes were highly heterogeneous from one patient to another, irrespective of MRI findings. Indeed, as it was previously described in patients with atypical inflammatory demyelinating lesion, most of the patients had evidence of a primary myelin disorder but a significant number (45%) had pathologic features suggestive of mild or sometimes marked astrocytic damage.

All our patients had preserved or increased AQP4 immunostaining. Previous autopsy studies have demonstrated conflicting results on AQP4 immunoreactivity in active MS lesions and AQP4-positive NMOSD; indeed, MS was initially supposed to be associated with preserved or increased AQP4 immunostaining whereas NMOSD lesions lack aquaporin-4 [16]. Nevertheless, these results were not confirmed in another autopsy study where AQP4 loss was observed in only 54% of NMOSD and conversely in 40% of MS patients [32]. Moreover, AQP4 immunostaining has been evaluated in a series of four autopsies of patients with Baló's lesions; it was systematically reduced [31]. In this context, it has been recently suggested that, in patients with AIIDL, AQP4 loss could be an important diagnostic aid since 18/20 (90%) patients had a decrease of AQP4 immunostaining suggestive of AQP4-positive NMOSD and 14 had AQP4-IgG in the serum [6]. Nevertheless, in that study, all the patients had pathologic findings supportive of a primary astrocytic disorder and most of them had spinal cord lesions. All the patients from our series had either monophasic AIIDL, MS or AQP4-negative NMOSD so that our results are difficult to compare with the study from Popescu et al. [6]. We rather suggest that, in unselected patients with active demyelinating lesion of the brain, AQP4 immunostaining is essentially preserved and thus argues against AQP4-positive NMOSD.

NMOSD criteria have been recently modified and now include symptomatic cerebral syndromes with NMOSD typical lesions [8]. Differential diagnosis between MS and NMOSD in patients presenting with a cerebral AIIDL can be difficult since almost all of these lesions have been described in NMOSD patients with and without AQP4 autoantibodies [4, 33]. Nevertheless, previous studies suggest that tumefactive, ring-like demyelinating lesions are more commonly found in MS, whereas NMOSD (either AQP4+ or AQP4−) has been mainly associated with infiltrative lesions [20, 34,

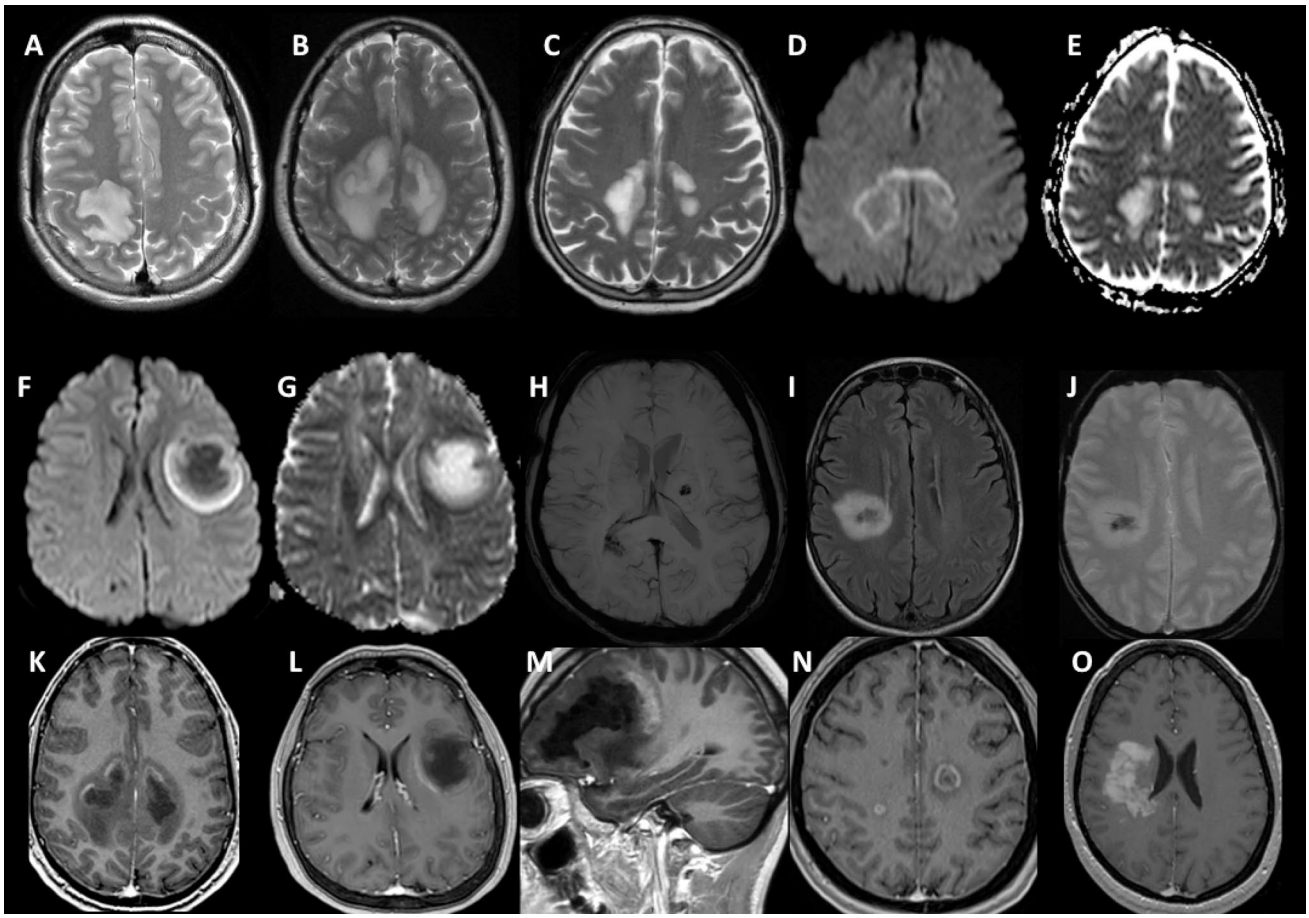

Fig. 2 Main MRI characteristics of the lesions. Main lesions were usually located in the juxtacortical white matter with few oedema/mass effect and rare cortical involvement (**a**). T2-weighted sequences only rarely identified a hypointense rim (**b**, **c**) as compared to a frequent hyperintense rim on diffusion-weighted images and a corresponding ADC decrease reflecting decrease diffusivity (**d**, **e**). This hyperintense rim could be associated with a hypointense core of the lesion with corresponding ADC increase (**f**, **g**). Susceptibility weighted imaging and T2* sequences identified a haemorrhagic component (**h**, **i**, **j**) even in some patients with a single lesion (**i**, **j**). Gadolinium enhancement was systematically seen (**k**–**o**) with common peripheral, open-rim enhancement (**k**, **l**, **m**) and more rarely concentric alternating rims (**n**) or central heterogeneous enhancement (**o**). MRI sequences are the following: T2 (**a**–**c**), B1000 (**d**, **f**), ADC (**e**, **g**), SWI (**h**), FLAIR (**i**), T2* (**j**) and post-gadolinium T1 (**k**–**o**)

35]. Our results seem to be in agreement with these findings since two of the three patients diagnosed with AQP4-negative NMOSD had an infiltrative lesion. Finally, we cannot rule out a disease associated with MOG autoantibodies since, due to the retrospective analysis, only 11 of the 20 patients were tested for MOG IgG. Nevertheless, none of our patients had the recently described fluffy lesions that have been found in patients with MOG IgG [36].

Overall, 16 patients (80%) had a monophasic atypical demyelinating lesion without recurrence and only four patients had a diagnosis of MS (one patient) or AQP4-negative NMOSD (three patients). This is not surprising since 75% of the patients from this series only had a single lesion confirming that, in patients with a cerebral demyelinating lesion, the absence of multiple lesions seems to predict the absence of recurrence [3, 9–11]. With respect to MS risk, only 1 patient had an MS diagnosis based on multiple lesions retrospectively considered to be typical of MS and fulfilling MS diagnostic criteria on initial MRI. Whether this low risk is related to the presence of immunomodulatory/suppressive treatment is not clear. Moreover, the relative short duration of follow-up in some patients does not rule out future development of MS. The identification of CSF-specific oligoclonal bands, albeit seen in the MS patient, was also identified in 1 AQP4-negative NMOSD patient and in 2 patients with monophasic disease.

The main limitations of our study include the retrospective design of the study (limiting us to perform additional pathological and MRI studies), the small number of patients, the absence of specific analysis of microglia/activated microglia and the absence of a blinded analysis of MRI. Moreover, it is important to underline that delay between clinical onset

Table 3 Histological characteristics of patients with active atypical demyelinating lesions

Patient	Cell infiltrate				Macrophages containing products		IgG deposits	Astrocytes morphology			Vascular hyalinization	Myelin vacuolation	Aqp-4 IHC	MRI pattern	Final diagnosis
	Macrophages	B cells	T cells	Granulocytes	Myelin	GFAP		Reactive	Dystrophic	Creutzfeldt–Peter Cells					
1[a]	+	−	−	−	+	−	+	+	−	+	−	−	+	Infiltrative	Unknown/rapid death
2[a]	+++	−	+	−	−	−	−	+	−	−	+	+	+	Other	Monophasic AIIDL
3	+++	−	−	−	+	−	+	+	+	+	−	−	+	Infiltrative	Monophasic AIIDL
4	+	−	+	−	−		−	+	−	−	−	−	+	Infiltrative	Monophasic AIIDL
5	+++	+	+	−	+		NA	+	−	+	+	−	+	Ring-like	Monophasic AIIDL
6	+++	+++	+	−	−	−	−	+	+	+	+	−	+	Infiltrative	NMOSD/severe left optic neuritis
7	+++	−	+	+	+	−	NA	+	+	−	−	−	+	AHLE	Monophasic AIIDL
8	+++	−	+	−	−	NA	−	−	−	−	−	−	+	Ring-like	Monophasic AIIDL
9[a]	+++	−	+	−	−	−	+	+	+	−	−	+	+	Balo-like	Monophasic AIIDL
10	+++	−	+	−	+	NA	+	+	+	−	−	−	+	Balo-like	Monophasic AIIDL
11	+++	+	+++	+	+	−	+	−	−	−	−	−	+	AHLE	Monophasic AIIDL
12	+++	−	+	−	−	−	−	+	+	+	−	−	+	Balo-like	MS/DIS + DIT at onset
13	+	−	−	−	+	−	+	+	+	−	−	−	+	Infiltrative	Monophasic AIIDL
14	+++	−	+	−	+	+	+	+	+	−	+	−	+	Infiltrative	NMOSD/severe recurrent right optic neuritis
15	+++	−	−	−	+	−	+	−	−	−	−	−	+	Infiltrative	Monophasic AIIDL
16[a]	+++	−	−	+	+	−	+	+	+	+	−	+	+	AHLE	Unknown/rapid death
17	+++	−	+	−	+	−	+	+	+	−	−	+	+	Ring-like	Monophasic AIIDL
18[a]	+++	−	+	−	+	−	+	+	+	−	−	+	+	Infiltrative	Monophasic AIIDL
19	+	+	+	+	+	−	−	+	+	+	−	+	+	AHLE	Monophasic AIIDL
20[a]	+++	−	−	−	+	−	−	+	−	−	−	−	+	Other	NMOSD/rapid death
Total	100%	20%	70%	20%	70%	6%	61%	85%	60%	35%	20%	30%	100%		

GFAP glial fibrillary acid protein, *Aqp-4* aquaporin-4, *IHC* immunohistochemistry, *MRI* magnetic resonance imaging, *AHLE* acute haemorrhagic leukoencephalitis, *NMOSD* Neuromyelitis optica spectrum disorder, *MS* multiple sclerosis

[a]Patients with steroids treatment given before pathological analysis

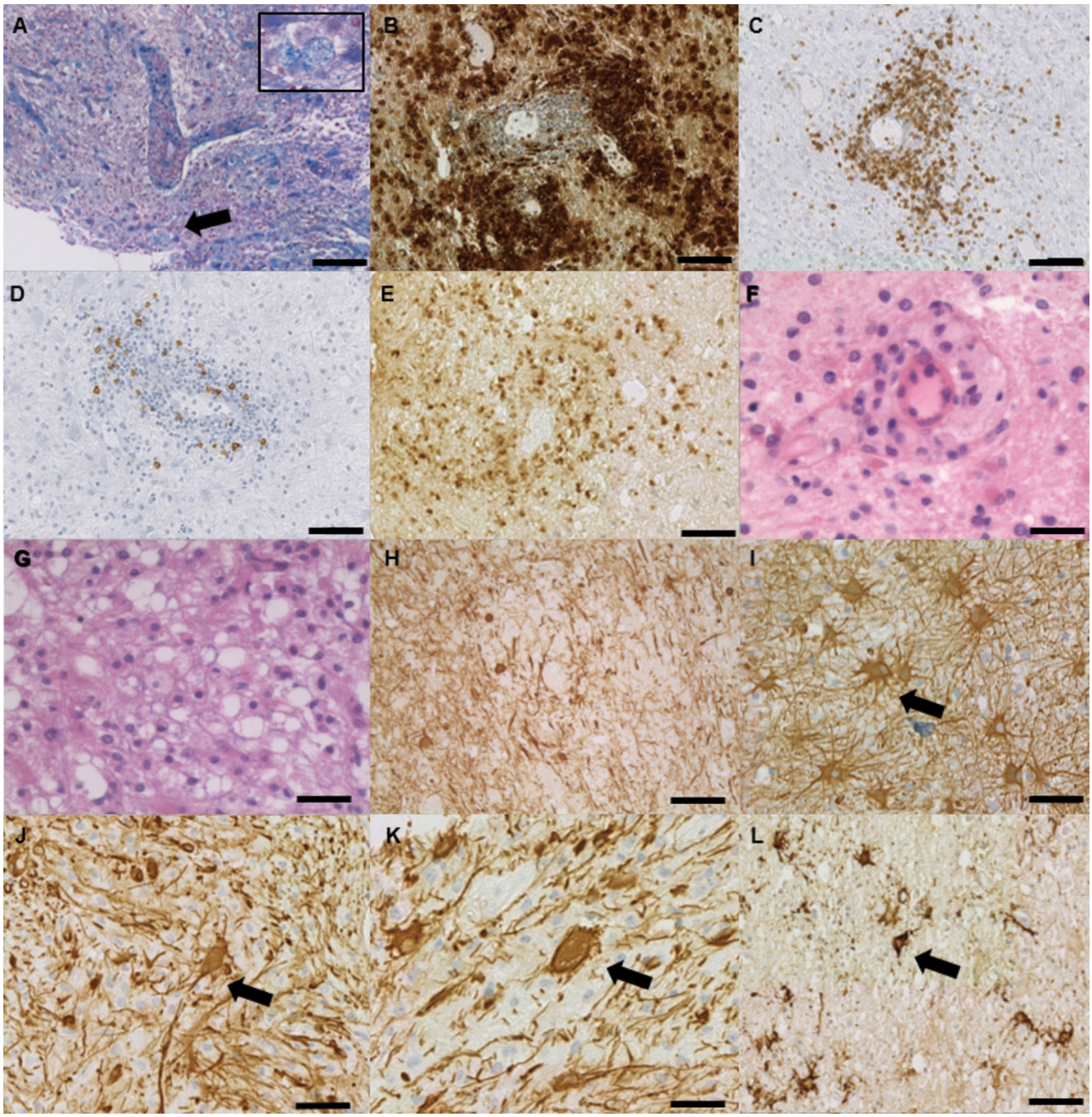

Fig. 3 Histological Characteristics. Histopathological analysis of patients' biopsies disclosed active demyelinating lesions. **a** Demyelination is seen (Luxol fast blue, scale bar = 100 μm) with macrophages containing myelin debris (arrow). **b**–**d** Inflammatory infiltrate is seen (scale bar = 100 μm) with (**b**) predominance of macrophages/microglia (CD68). **c** T cells infiltrate is less pronounced (CD3) and **d** B cells are rarely seen (CD20). **e** IgG deposits are frequent (IgG, scale bar = 50 μm). Vascular hyalinization (**f** scale bar = 33 μm), myelin and vacuolation (**g** scale bar = 50 μm) are found in a variable proportion of patients. Neurons are relatively preserved (**h** Neurofilaments, scale bar = 50 μm). Astrocytes pathology disclosed preserved/increased GFAP (**i**–**k**) and AQP4 staining (**l**). Reactive astrocytes are found in all the lesions (**i** arrow, scale bar = 50 μm). Small GFAP (**j** arrow, scale bar = 33 μm) and AQP4 positive (**l** arrow, scale bar = 100 μm) dystrophic astrocytes are frequently identified whereas Creutzfeldt–Peters cells with abundant cytoplasm and fragmented nuclear inclusions are more rarely seen (**k** arrow, scale bar = 33 μm)

and MRI and pathological evaluation as well as an ongoing steroid treatment at the time of the biopsy in six patients could have largely influenced MRI and/or pathological results. This is probably one of the most important limitations of the study.

To conclude, in spite of the marked heterogeneity of brain AIIDL, our study confirms that some common features such as peripheral DWI hyperintense rim with open-rim enhancement and absence of oedema are clearly suggestive of a demyelinating lesion and thus should preclude brain biopsy. We also confirm that, whatever the radiologic characteristics of the atypical demyelinating lesions are, pathologic changes are heterogeneous. Despite the identification of sometimes marked astrocytic changes, AQP4 staining on immunohistochemistry is systematically retained in brain AIIDL and argues against AQP4-positive NMOSD. Finally, we confirm that, in spite of a potentially dramatic initial evolution, patients with a first episode of AIIDL have a low risk of recurrence.

Author contribution XA: study concept and design, acquisition of data, analysis and interpretation, and writing. VR: laboratory analysis, critical revision of the manuscript for important intellectual content. BL: laboratory analysis, critical revision of the manuscript for important intellectual content. TV: laboratory analysis, critical revision of the manuscript for important intellectual content. NMdeC: acquisition of data, critical revision of the manuscript for important intellectual content. CC-D: acquisition of data, critical revision of the manuscript for important intellectual content. MC: acquisition of data, critical revision of the manuscript for important intellectual content. NC: acquisition of data, critical revision of the manuscript for important intellectual content. JdeS: acquisition of data, critical revision of the manuscript for important intellectual content. SH: acquisition of data, critical revision of the manuscript for important intellectual content. GA: acquisition of data, critical revision of the manuscript for important intellectual content. HO: acquisition of data, critical revision of the manuscript for important intellectual content. FC: acquisition of data, critical revision of the manuscript for important intellectual content. FD-D: acquisition of data, critical revision of the manuscript for important intellectual content. RM: acquisition of data, critical revision of the manuscript for important intellectual content. FT: acquisition of data, critical revision of the manuscript for important intellectual content. MC: acquisition of data, critical revision of the manuscript for important intellectual content. A-MG: acquisition of data, critical revision of the manuscript for important intellectual content. AK: acquisition of data, critical revision of the manuscript for important intellectual content. GE: acquisition of data, critical revision of the manuscript for important intellectual content. BC-N, TA: acquisition of data, critical revision of the manuscript for important intellectual content. DS: acquisition of data, critical revision of the manuscript for important intellectual content. ET: acquisition of data, critical revision of the manuscript for important intellectual content. AR: acquisition of data, critical revision of the manuscript for important intellectual content. LM: acquisition of data, critical revision of the manuscript for important intellectual content. M-P, B-M: acquisition of data, critical revision of the manuscript for important intellectual content. PL: study concept and design, acquisition of data, critical revision of the manuscript for important intellectual content. SK: study concept and design, acquisition of data, analysis and interpretation, critical revision of the manuscript for important intellectual content.

Compliance with ethical standards

Conflicts of interest Xavier Ayrignac has received consulting and lecturing fees, travel grants and research support from Bayer-Schering, Biogen Idec, Genzyme, Novartis, Merck Serono, Roche, and Teva Pharma. Valérie Rigau reports no disclosure relevant to this manuscript. Benoit Lhermitte reports no disclosure relevant to this manuscript. Thierry Vincent reports no disclosure relevant to this manuscript. Nicolas Menjot de Champfleur reports no disclosure relevant to this manuscript. Clarisse Carra-Dalliere reports no disclosure relevant to this manuscript. Mahmoud Charif reports no disclosure relevant to this manuscript. Nicolas Collongues reports no disclosure relevant to this manuscript. Jérôme de Seze reports no disclosure relevant to this manuscript. Sonia Hebbadj reports no disclosure relevant to this manuscript. Guido Ahle reports no disclosure relevant to this manuscript. Hélène Oesterlé reports no disclosure relevant to this manuscript. François Cotton reports no disclosure relevant to this manuscript. Françoise Durand-Dubief reports no disclosure relevant to this manuscript. Romain Marignier serves on scientific advisory board for MedImmune and has received funding for travel and honoraria from Biogen Idec, Merck Serono, Novartis, Sanofi-Genzyme and Teva. Frédéric Taithe reports no disclosure relevant to this manuscript. Mikael Cohen reports no disclosure relevant to this manuscript. Anne-Marie Guennoc reports no disclosure relevant to this manuscript. Anne Kerbrat reports no disclosure relevant to this manuscript. Gilles Edan reports no disclosure relevant to this manuscript. Béatrice Carsin-Nicol reports no disclosure relevant to this manuscript. Thibaut Allou reports no disclosure relevant to this manuscript. Denis Sablot reports no disclosure relevant to this manuscript. Eric Thouvenot reports no disclosure relevant to this manuscript. Aurélie Ruet or her institution received research grants and/or consulting fees from Novartis, Biogen, Merck-Serono, Bayer Healthcare, Roche, Teva, and Genzyme unrelated to the submitted work. Laurent Magy has received Honoraria, housing and consultancies from CSL Behring, Biogen, Teva Pharma, Octapharma, Pharnext, Sanofi Genzyme, Novartis. Marie-Paule Boncoeur-Martel reports no disclosure relevant to this manuscript. Pierre Labauge reports no disclosure relevant to this manuscript. Stéphane Kremer reports no disclosure relevant to this manuscript.

Ethics approval The study was approved by Montpellier University Hospital Ethical Committee (Q-2017-03-02) and was registered on ClinicalTrial.gov (NCT03121105).

References

1. Hardy TA, Reddel SW, Barnett MH et al (2016) Atypical inflammatory demyelinating syndromes of the CNS. Lancet Neurol 15:967–981. https://doi.org/10.1016/S1474-4422(16)30043-6
2. Hardy TA, Miller DH (2014) Baló's concentric sclerosis. Lancet Neurol 13:740–746. https://doi.org/10.1016/S1474-4422(14)70052-3
3. Hardy TA, Chataway J (2013) Tumefactive demyelination: an approach to diagnosis and management. J Neurol Neurosurg Psychiatry 84:1047–1053. https://doi.org/10.1136/jnnp-2012-304498
4. Uehara T, Beck G, Baba K et al (2016) Tumefactive brain lesion with rapid cavity formation associated with anti-aquaporin-4 antibody. Neurol Neuroimmunol Neuroinflammation 3:e230. https://doi.org/10.1212/NXI.0000000000000230
5. Wang JJ, Jaunmuktane Z, Mummery C et al (2016) Inflammatory demyelination without astrocyte loss in MOG antibody-positive NMOSD. Neurology 87:229–231. https://doi.org/10.1212/WNL.0000000000002844
6. Popescu BFG, Guo Y, Jentoft ME et al (2015) Diagnostic utility of aquaporin-4 in the analysis of active demyelinating lesions. Neurology 84:148–158. https://doi.org/10.1212/WNL.0000000000001126

7. Polman CH, Reingold SC, Banwell B et al (2011) Diagnostic criteria for multiple sclerosis: 2010 revisions to the McDonald criteria. Ann Neurol 69:292–302. https://doi.org/10.1002/ana.22366
8. Wingerchuk DM, Banwell B, Bennett JL et al (2015) International consensus diagnostic criteria for neuromyelitis optica spectrum disorders. Neurology 85:177–189. https://doi.org/10.1212/WNL.0000000000001729
9. Siri A, Carra-Dalliere C, Ayrignac X et al (2015) Isolated tumefactive demyelinating lesions: diagnosis and long-term evolution of 16 patients in a multicentric study. J Neurol 262:1637–1645. https://doi.org/10.1007/s00415-015-7758-8
10. Lucchinetti CF, Gavrilova RH, Metz I et al (2008) Clinical and radiographic spectrum of pathologically confirmed tumefactive multiple sclerosis. Brain J Neurol 131:1759–1775. https://doi.org/10.1093/brain/awn098
11. Jeong IH, Kim S-H, Hyun J-W et al (2015) Tumefactive demyelinating lesions as a first clinical event: clinical, imaging, and follow-up observations. J Neurol Sci 358:118–124. https://doi.org/10.1016/j.jns.2015.08.034
12. Seewann A, Enzinger C, Filippi M et al (2008) MRI characteristics of atypical idiopathic inflammatory demyelinating lesions of the brain: a review of reported findings. J Neurol 255:1–10. https://doi.org/10.1007/s00415-007-0754-x
13. Kuhlmann T, Ludwin S, Prat A et al (2017) An updated histological classification system for multiple sclerosis lesions. Acta Neuropathol (Berl) 133:13–24. https://doi.org/10.1007/s00401-016-1653-y
14. Brück W, Popescu B, Lucchinetti CF et al (2012) Neuromyelitis optica lesions may inform multiple sclerosis heterogeneity debate. Ann Neurol 72:385–394. https://doi.org/10.1002/ana.23621
15. Misu T, Fujihara K, Kakita A et al (2007) Loss of aquaporin 4 in lesions of neuromyelitis optica: distinction from multiple sclerosis. Brain J Neurol 130:1224–1234. https://doi.org/10.1093/brain/awm047
16. Roemer SF, Parisi JE, Lennon VA et al (2007) Pattern-specific loss of aquaporin-4 immunoreactivity distinguishes neuromyelitis optica from multiple sclerosis. Brain J Neurol 130:1194–1205. https://doi.org/10.1093/brain/awl371
17. Altintas A, Petek B, Isik N et al (2012) Clinical and radiological characteristics of tumefactive demyelinating lesions: follow-up study. Mult Scler Houndmills Basingstoke Engl 18:1448–1453. https://doi.org/10.1177/1352458512438237
18. Koelblinger C, Fruehwald-Pallamar J, Kubin K et al (2013) Atypical idiopathic inflammatory demyelinating lesions (IIDL): conventional and diffusion-weighted MR imaging (DWI) findings in 42 cases. Eur J Radiol 82:1996–2004. https://doi.org/10.1016/j.ejrad.2013.07.026
19. Hiremath SB, Muraleedharan A, Kumar S et al (2017) Combining diffusion tensor metrics and DSC perfusion imaging: can it improve the diagnostic accuracy in differentiating tumefactive demyelination from high-grade glioma? AJNR Am J Neuroradiol 38:685–690. https://doi.org/10.3174/ajnr.A5089
20. Wallner-Blazek M, Rovira A, Fillipp M et al (2013) Atypical idiopathic inflammatory demyelinating lesions: prognostic implications and relation to multiple sclerosis. J Neurol 260:2016–2022. https://doi.org/10.1007/s00415-013-6918-y
21. Renard D, Castelnovo G, Campello C et al (2014) An MRI review of acquired corpus callosum lesions. J Neurol Neurosurg Psychiatry 85:1041–1048. https://doi.org/10.1136/jnnp-2013-307072
22. Garg N, Reddel SW, Miller DH et al (2015) The corpus callosum in the diagnosis of multiple sclerosis and other CNS demyelinating and inflammatory diseases. J Neurol Neurosurg Psychiatry 86:1374–1382. https://doi.org/10.1136/jnnp-2014-309649
23. Lu S-S, Kim SJ, Kim HS et al (2014) Utility of proton MR spectroscopy for differentiating typical and atypical primary central nervous system lymphomas from tumefactive demyelinating lesions. AJNR Am J Neuroradiol 35:270–277. https://doi.org/10.3174/ajnr.A3677
24. Toh CH, Wei K-C, Chang C-N et al (2013) Differentiation of primary central nervous system lymphomas and glioblastomas: comparisons of diagnostic performance of dynamic susceptibility contrast-enhanced perfusion MR imaging without and with contrast-leakage correction. AJNR Am J Neuroradiol 34:1145–1149. https://doi.org/10.3174/ajnr.A3383
25. Kim DS, Na DG, Kim KH et al (2009) Distinguishing tumefactive demyelinating lesions from glioma or central nervous system lymphoma: added value of unenhanced CT compared with conventional contrast-enhanced MR imaging. Radiology 251:467–475. https://doi.org/10.1148/radiol.2512072071
26. Hu W, Lucchinetti CF (2009) The pathological spectrum of CNS inflammatory demyelinating diseases. Semin Immunopathol 31:439–453. https://doi.org/10.1007/s00281-009-0178-z
27. Mandler RN, Davis LE, Jeffery DR, Kornfeld M (1993) Devic's neuromyelitis optica: a clinicopathological study of 8 patients. Ann Neurol 34:162–168. https://doi.org/10.1002/ana.410340211
28. Takano R, Misu T, Takahashi T et al (2010) Astrocytic damage is far more severe than demyelination in NMO: a clinical CSF biomarker study. Neurology 75:208–216. https://doi.org/10.1212/WNL.0b013e3181e2414b
29. Morales Y, Parisi JE, Lucchinetti CF (2006) The pathology of multiple sclerosis: evidence for heterogeneity. Adv Neurol 98:27–45
30. Ando M, Yamashiro K, Noda K, Okuma Y (2011) Aquaporin-4 autoimmunity can cause exclusive brain tumefactive lesions. Intern Med Tokyo Jpn 50:2437–2438
31. Matsuoka T, Suzuki SO, Iwaki T et al (2010) Aquaporin-4 astrocytopathy in Baló's disease. Acta Neuropathol (Berl) 120:651–660. https://doi.org/10.1007/s00401-010-0733-7
32. Matsuoka T, Suzuki SO, Suenaga T et al (2011) Reappraisal of aquaporin-4 astrocytopathy in Asian neuromyelitis optica and multiple sclerosis patients. Brain Pathol Zurich Switz 21:516–532. https://doi.org/10.1111/j.1750-3639.2011.00475.x
33. Masuda H, Mori M, Katayama K et al (2013) Anti-aquaporin-4 antibody-seronegative NMO spectrum disorder with Baló's concentric lesions. Intern Med Tokyo Jpn 52:1517–1521
34. Fargeot G, Aboab J, Savatovsky J et al (2018) Central nervous system Aquaporin4 autoimmunity revealed by a single pseudotumoral encephalic lesion. Metab Brain Dis 33:353–355. https://doi.org/10.1007/s11011-017-0141-y
35. Kim S-H, Kim W, Kook M-C et al (2012) Central nervous system aquaporin-4 autoimmunity presenting with an isolated cerebral abnormality. Mult Scler Houndmills Basingstoke Engl 18:1340–1343. https://doi.org/10.1177/1352458512441271
36. Jurynczyk M, Geraldes R, Probert F et al (2017) Distinct brain imaging characteristics of autoantibody-mediated CNS conditions and multiple sclerosis. Brain J Neurol 140:617–627. https://doi.org/10.1093/brain/aww350

Affiliations

Xavier Ayrignac[1,2] · Valérie Rigau[3] · Benoit Lhermitte[4] · Thierry Vincent[5] · Nicolas Menjot de Champfleur[6] · Clarisse Carra-Dalliere[1] · Mahmoud Charif[1] · Nicolas Collongues[7] · Jérôme de Seze[7] · Sonia Hebbadj[8] · Guido Ahle[9] · Hélène Oesterlé[10] · François Cotton[11] · Françoise Durand-Dubief[12] · Romain Marignier[12] · Sandra Vukusic[12] · Frédéric Taithe[13] · Mikael Cohen[14] · Anne-Marie Guennoc[15] · Anne Kerbrat[16] · Gilles Edan[16] · Béatrice Carsin-Nicol[17] · Thibaut Allou[18] · Denis Sablot[18] · Eric Thouvenot[19] · Aurélie Ruet[20] · Laurent Magy[21] · Marie-Paule Boncoeur-Martel[22] · Pierre Labauge[1] · Stéphane Kremer[8]

1 Department of Neurology, Multiple Sclerosis Center, Montpellier University Hospital, 80 rue Augustin Fliche, 34295 Montpellier, Cedex 05, France

2 The Institute for Neurosciences of Montpellier, Inserm UMR1051, Saint Eloi Hospital, University of Montpellier, Montpellier, France

3 Department of Pathology, Montpellier University Hospital, Montpellier, France

4 Department of Pathology, Strasbourg University Hospital, Strasbourg, France

5 Department of Immunology, Montpellier University Hospital, Montpellier, France

6 Department of Neuroradiology, Montpellier University Hospital, Montpellier, France

7 Department of Neurology and Clinical Investigation Center, Strasbourg University Hospital, Strasbourg, France

8 Department of Radiology, Strasbourg University Hospital, Strasbourg, France

9 Department of Neurology, Colmar Hospital, Colmar, France

10 Department of Pathology, Colmar Hospital, Colmar, France

11 Department of Radiology, Centre hospitalier Lyon-Sud, hospices civils de Lyon, Lyon, France

12 Department of Neurology, Hôpital Neurologique Pierre Wertheimer Hospices Civils de Lyon, Lyon, France

13 Department of Neurology, Clermont-Ferrand University Hospital, Clermont-Ferrand, France

14 Department of Neurology, Nice University Hospital, Nice, France

15 Department of Neurology, Tours University Hospital, Tours, France

16 Department of Neurology, Rennes University Hospital, Rennes, France

17 Department of Neuroradiology, Rennes University Hospital, Rennes, France

18 Department of Neurology, Perpignan Hospital, Perpignan, France

19 Department of Neurology, Nimes University Hospital, Nîmes, France

20 Department of Neurology, Bordeaux University Hospital, Bordeaux, France

21 Department of Neurology, Limoges University Hospital, Limoges, France

22 Department of Neuroradiology, Limoges University Hospital, Limoges, France